IOP Publishing Journal of Physics B: Atomic, Molecular and Optical Physics
J. Phys. B: At. Mol. Opt. Phys. **55** (2022) 025201 (12pp) https://doi.org/10.1088/1361-6455/ac37f3

Low energy inelastic electron scattering from carbon monoxide: II. Excitation of the $b^3\Sigma^+$, $j^3\Sigma^+$, $B^1\Sigma^+$, $C^1\Sigma^+$ and $E^1\Pi$ Rydberg electronic states

Mateusz Zawadzki[1,2], Murtadha A Khakoo[1,*], Ahmad Sakaamini[1], Logan Voorneman[1], Luka Ratkovich[1], Zdeněk Mašín[3], Amar Dora[4], Russ Laher[5] and Jonathan Tennyson[6]

[1] Physics Department, California State University, Fullerton CA 92831, United States of America
[2] Atomic Physics Division, Department of Atomic, Molecular and Optical Physics, Gdańsk University of Technology, ul. G. Narutowicza 11/12, 80-233 Gdańsk, Poland
[3] Institute of Theoretical Physics, Faculty of Mathematics and Physics, Charles University, V Holešovičkách 2, 180 00, Prague 8, Czech Republic
[4] Department of Chemistry, North Orissa University, Baripada-757 003, Mayurbhanj, Odisha, India
[5] NASA Exoplanet Science Institute, California Institute of Technology, 1200 E. California Blvd, Pasadena, CA 91125, United States of America
[6] Department of Physics and Astronomy, University College London, London WC1E 6BT, United Kingdom

E-mail: mkhakoo@fullerton.edu

Received 8 August 2021, revised 27 October 2021
Accepted for publication 9 November 2021
Published 10 February 2022

Abstract

In this second part of a two part paper (first part: Zawadzki *et al* (2020 *J. Phys. B: At. Mol. Opt. Phys.* **53** 165201)) we present differential scattering cross sections for excitation of several Rydberg electronic states of carbon monoxide by electron impact. The first part concerned the low-lying valence states of CO. In the present study cross sections are obtained experimentally using low-energy electron energy-loss spectroscopy and theoretically using the R-matrix method. Incident electron energies range from near-threshold of 12.5 eV to 20 eV while the scattering angles range from 20° to 120°. The R-matrix calculations use three distinct close-coupling models and their results are compared to available experimental and theoretical cross sections. The overall comparison leads to significantly improved description of the excitation cross sections for this target.

Keywords: inelastic, electron, scattering, carbon monoxide, R-matrix

(Some figures may appear in colour only in the online journal)

1. Introduction

Carbon Monoxide is the most abundant molecule after H_2 and is one of the main components of the atmosphere of Venus and Mars (Campbell *et al* 2011). In optical spectroscopy the $^2\Sigma$–$^2\Pi$ comet-tail bands of CO, at the wavelength of 438 nm, are most prominently observed in the astrophysical phenomena (Huber and Herzberg 1950) dealing with comets. In addition, CO is used in discharges for various applications (Sakurai and Yokoyama 2000). CO is also used in fuel gas mixtures with hydrogen and other gases for industrial and domestic heating (Ghenai 2010) and chemically in the manufacture of a variety of chemicals such as acids, esters and alcohols (Nakano *et al* 2009) as well as in fuel cells (Kaltschmitt and Deutschmann 2012).

* Author to whom any correspondence should be addressed.

In a previous paper designated as (I) (Zawadzki *et al* 2020), we investigated the differential electron impact excitation of the lower lying valence $a^3\Pi$, $a'^3\Sigma^+$ and $A^1\Pi$ electronic states of CO from a near-threshold incident electron energy (E_0) of 6.3 eV to an incident energy of 20 eV and for electron scattering angles (θ) of 10° to 120°, using a well-tested high-resolution electron spectrometer. In that paper, the electron energy loss spectra of CO were unfolded to extract the component full-electronic excitation (i.e. summed over all vibrational levels) of the above valence electronic bands. In this follow-up paper designated as (II) we extend the study of the electronic excitations of the valence bands in (I) to the $b^3\Sigma^+$, $j^3\Sigma^+$, $B^1\Sigma^+$, $C^1\Sigma^+$ and $E^1\Pi$ Rydberg electronic states. Here the E_0 range is from 12.5 eV to 20 eV for the same range of θ. The excitation of the electronic states observed in our spectra, whose energy loss span was from 5.75 eV to 11.75 eV, covered the excitation of the $a^3\Pi$, $a'^3\Sigma^+$, $d^3\Delta$, $e^3\Sigma$, $I^1\Sigma^-$, $D^1\Delta$, $A^1\Pi$, $b^3\Sigma^+$, $B^1\Sigma^+$, $j^3\Sigma^+$, $C^1\Sigma^+$ and $E^1\Pi$ electronic states. However, unfolding these spectra systematically resulted in unfolding groups of these states: $a^3\Pi$, $a'^3\Sigma^+$, $d^3\Delta + e^3\Sigma + I^1\Sigma^- + D^1\Delta$, $A^1\Pi$, $b^3\Sigma^+$, $B^1\Sigma^+$, $j^3\Sigma^+$, $C^1\Sigma^+$ and $E^1\Pi$ components, i.e. summations of state cross sections where individual separation of their excitation was not possible.

Experimental work on differential cross sections (DCSs) for excitation of the Rydberg electronic states of CO, was made initially by Mazeau *et al* (1975) who measured relative DCSs for excitation of the $b^3\Sigma^+$ and $B^1\Sigma^+$ states. Swanson *et al* (1975) reported relative differential excitation functions for the $b^3\Sigma^+$, $B^1\Sigma^+$, $C^1\Sigma^+$, $c^3\Pi$, $E^1\Pi$ at θ of 45°. Allan (1989) also reported relative excitation functions for the $b^3\Sigma^+$, $B^1\Sigma^+$ and $j^3\Sigma^+$ states using a trochoidal spectrometer at extreme θ values of 0° and 180°. Middleton *et al* (1993) determined DCSs for excitation of the $a^3\Pi$, $a'^3\Sigma^+$, $d^3\Delta + e^3\Sigma + I^1\Sigma^- + D^1\Delta$, $A^1\Pi$, $b^3\Sigma^+$, $B^1\Sigma^+$, $j^3\Sigma^+$, $C^1\Sigma^+ + c^3\Pi$ and $E^1\Pi$ states of CO at E_0 values of 20 eV, 30 eV, 40 eV and 50 eV at θ values of 10° to 90°, using unfolded electron energy loss spectra following the scheme used similarly by Cartwright *et al* (1977) for differential electron impact excitation of N_2. Note that the DCSs for individual and summed excitations were presented. Zobel *et al* (1995) measured DCSs for excitation of the $b^3\Sigma^+$, $B^1\Sigma^+$, $C^1\Sigma^+$, and $E^1\Pi$ Rydberg states of CO at various incident E_0 values from 0.1 eV to 3.7 eV above threshold. Zobel *et al* (1996) followed this by similar work on the $a^3\Pi$, $a'^3\Sigma^+$, $d^3\Delta$ and $A^1\Pi$ valence states at various incident E_0 values from 0.1 eV to 3.7 eV above threshold for θ values from 20° to 140°. Zetner *et al* (1998) measured DCSs at the E_0 values of 10 eV, 12.5 eV and 15 eV for θ values of 9° to 134° and compared their results with those of Zobel *et al* (1995) and obtained very good agreement in these comparisons.

The reader is strongly referred to the most recent and comprehensive review of electron impact cross sections for CO by Itikawa (2015) which covers total scattering cross sections, elastic scattering cross sections, integral and momentum transfer scattering cross sections, rotation and vibrational excitation and electronic excitation cross sections for the $a^3\Pi$, $a'^3\Sigma^+$, $b^3\Sigma^+$, $A^1\Pi$, $B^1\Sigma^+$, $C^1\Sigma^+$ and $E^1\Pi$ states as well as ionization cross sections of CO; Itikawa thus updates earlier reviews given by Brunger and Buckman (2002) and Trajmar *et al* (1983) for electron scattering from CO. Itikawa (2015) also gives recommended values of integral elastic, momentum transfer, excitation and ionization cross sections for CO. As was found in (I) (Zawadzki *et al* 2020) there existed a paucity of full-electronic state cross sections for excitation of the Rydberg states of CO over an extended energyrange to be of use for comprehensive data for modeling studies. With this situation in mind we have decided to study the CO energy loss spectrum for the higher lying Rydberg states too and for energies ranging from near threshold (in this case 12.5 eV) up to 20 eV. The experimental method used is identical to that described in (I) (Zawadzki *et al* 2020). The DCSs here were taken for the $b^3\Sigma^+$, $j^3\Sigma^+$, $B^1\Sigma^+$, $C^1\Sigma^+$ and $E^1\Pi$ Rydberg electronic states for E_0 values of 12.5 eV, 15 eV, 17.5 eV and 20 eV for θ values of 10° to 120°. The experimental results are similarly compared to present more sophisticated R-matrix calculations for excitation of these Rydberg states. The present experimental and theoretical approaches are described in the following sections.

2. Experimental approach

The experimental method used here had already been detailed in (I) (Zawadzki *et al* 2020). Thus only a brief account of the experiment will be given here. The apparatus has been described in earlier papers (Khakoo *et al* 1994, Varela *et al* 2015, Ralphs *et al* 2013). The electron spectrometer has been well-tested and has 2.54 cm titanium cylindrical lenses with double hemispheres both in the monochromator and analyzer. The device operates with a resolution of 33 meV to 40 meV with an incident electron current of 7 to 10 nA. The analyser could be rotated about the collision center over the θ range up to 120°. The angular resolution was 2.5°, full-width at half-maximum, and was housed in a shielded vacuum chamber with a residual magnetic field of ≈2 mG. The chamber ran at a base pressure of 1×10^{-7} torr and typically rose to 4×10^{-6} torr when CO gas was admitted via a collimated aperture gas target source into the system at a drive pressure of 0.8 torr. This collimated source of CO could be rotated in and out of the collision region to determine accurate electron scattering backgrounds (Hughes *et al* 2003). The spectrometer was baked by biaxial heating wire, which did not contribute to the magnetic field in the chamber, to a temperature of ≈100 °C to stabilise the spectrometer surfaces over a long term. Electron energy loss spectra in the energy loss range of −0.150 eV sweeping to 0.150 eV and then jumping to 5.750 eV and sweeping to 11.750 eV (step size 6.36 mV/bin) were taken using multichannel scaling methods as described in (I) (Zawadzki *et al* 2020). Typically a minimum of two energy loss spectra were taken at any E_0 and θ. These spectra were fitted using linear and non-linear least-squares fits using algorithms obtained from numerical recipes (Press *et al* 1988), with Franck–Condon based electronic state envelopes as well as individual (vibrational) lines and using steps discussed in detail in (I) (Zawadzki *et al* 2020). The Franck–Condon factors used are listed in table 2 of (I)

Table 1. Vertical excitation energies of the Rydberg electronic excited states of CO studied in this work; experimental data are from (Huber and Herzberg 1979). The columns UKRmol and UKRmol+ contain data generated by the model constructed in paper I (Zawadzki *et al* 2020). The UKRmol model used the active space (6, 3, 3, 0) and a compact basis set cc-pV6Z while UKRmol+ used the active space (6, 2, 2, 0) and the basis set cc-pVQZ. Models 7330 and 9440, which were constructed in this work, both used the same diffuse atomic basis set aug-cc-pVQZ and active spaces (7, 3, 3, 0) and (9, 4, 4, 0) respectively.

State	Experiment	UKRmol	UKRmol+	Model 7330	Model 9440
B $^1\Sigma^+$	10.78	11.16	10.70	10.48	10.45
C $^1\Sigma^+$	11.40	14.93	16.95	11.13	10.70
b $^3\Sigma^+$	10.40	10.39	9.90	9.63	9.48
j $^3\Sigma^+$	11.30	14.25	20.70	10.15	10.24
E $^1\Pi$	11.53	11.84	14.68	11.17	13.31

Table 2. Present experimental DCS, ICS and MTCS for excitation of the $b^3\Sigma^+$ state in units of 10^{-18} cm^2/sr and cm^2.

θ (°)	E_0 (eV)							
	12.5 eV	Error	15 eV	Error	17.5 eV	Error	20 eV	Error
10			0.507	0.134	0.330	0.083	0.345	0.096
15	0.584	0.136	0.481	0.124	0.304	0.075	0.337	0.092
20	0.510	0.114	0.368	0.091	0.293	0.069	0.298	0.078
25	0.493	0.114	0.324	0.083	0.235	0.058	0.300	0.081
30	0.441	0.104	0.325	0.084	0.231	0.057	0.286	0.078
40	0.430	0.109	0.287	0.080	0.252	0.068	0.243	0.072
50	0.345	0.083	0.227	0.060	0.243	0.062	0.233	0.065
60	0.321	0.075	0.205	0.053	0.243	0.061	0.226	0.062
70	0.332	0.078	0.210	0.055	0.246	0.062	0.227	0.062
80	0.253	0.062	0.179	0.048	0.256	0.066	0.189	0.054
90	0.202	0.050	0.224	0.061	0.243	0.063	0.202	0.058
100	0.185	0.046	0.191	0.053	0.277	0.074	0.267	0.078
110	0.193	0.049	0.238	0.067	0.289	0.078	0.270	0.080
120	0.165	0.042	0.265	0.075	0.371	0.100	0.324	0.097
ICS	3.38	0.89	3.28	0.86	3.49	0.92	3.44	0.90
MTCS	2.71	0.71	3.37	0.89	3.94	1.04	3.73	0.98

(Zawadzki *et al* 2020). During the course of the fittings, the resulting analysis of the spectra were also corrected for transmission effects using He conventional electrostatic energy loss spectra and N_2 electron time-of-flight energy loss spectra (see discussion in I) and using these to normalise our transmission-corrected energy loss spectra to the elastic scattering peak in these spectra taken along with the inelastic spectra. The elastic peak was normalised to the elastic scattering DCSs of Gibson *et al* (1996) in turn to obtain normalised DCSs for the inelastic features. As discussed in I, the Gibson *et al* (1996) DCSs were chosen because they nicely covered the E_0 range of the present measurements and could be accurately interpolated for all the present E_0 and θ values, as well as being in very good agreement with the corrected elastic DCSs of Tanaka *et al* (1978) (that were corrected by Trajmar *et al* (1983) for He normalisation). The normalised inelastic scattering DCSs comprised of the $a^3\Pi$, $a'^3\Sigma^+$, $d^3\Delta + e^3\Sigma + I^1\Sigma^- + D^1\Delta$, $A^1\Pi$, $b^3\Sigma^+$, $B^1\Sigma^+$, $j^3\Sigma^+$, $C^1\Sigma^+$ and $E^1\Pi$ components, where the summations refer to states which could not be separated in the fitting. The valence $a^3\Pi$, $a'^3\Sigma^+$ and $A^1\Pi$ DCSs were presented in (I) Zawadzki *et al* (2020). The present work thus deals selectively with the excitation of Rydberg states $b^3\Sigma^+$, $B^1\Sigma^+$, $j^3\Sigma^+$, $C^1\Sigma^+$ and $E^1\Pi$.

3. Theory

As in paper (I), the theoretical results reported here are based on R-matrix calculations using both the standard UKRMol code (Carr *et al* 2012) and the newer heavily upgraded UKRMol+ code (Mašín *et al* 2020). While the UKRMol code can only use Gaussian type orbitals (GTOs) to represent the continuum functions and allow stable calculations for smaller R-matrix sphere size of radius up to $a = 15$ Bohr, the UKRMol+ code can use both GTOs and B-splines and therefore allows R-matrix spheres of arbitrarily large radii. This capability of UKRMol+ code has significant advantage over the UKRMol code in that it can be used to study larger molecules, molecules at longer bond lengths and for calculations that use diffuse atomic basis functions to represent Rydberg electronic states of target molecule. This later capability

Table 3. Present experimental DCS, ICS and MTCS for excitation of the $B^1\Sigma^+$ state in units of 10^{-18} cm^2/sr and cm^2.

θ (°)	E_0 (eV)							
	12.5 eV	Error	15 eV	Error	17.5 eV	Error	20 eV	Error
10			3.37	1.25	1.47	0.28	1.30	0.247
15	2.68	0.85	2.20	0.51	0.994	0.189	0.882	0.168
20	1.40	0.45	1.36	0.30	0.815	0.155	0.779	0.148
25	1.24	0.25	0.981	0.167	0.615	0.117	0.780	0.148
30	0.716	0.136	0.863	0.147	0.574	0.109	0.811	0.154
40	0.439	0.083	0.611	0.104	0.653	0.124	0.664	0.126
50	0.299	0.057	0.440	0.075	0.497	0.094	0.662	0.126
60	0.258	0.049	0.400	0.068	0.444	0.084	0.454	0.086
70	0.231	0.044	0.328	0.056	0.391	0.074	0.404	0.077
80	0.194	0.037	0.418	0.071	0.255	0.048	0.263	0.050
90	0.132	0.025	0.338	0.057	0.269	0.051	0.318	0.060
100	0.148	0.028	0.423	0.072	0.377	0.072	0.356	0.068
110	0.159	0.030	0.461	0.078	0.380	0.072	0.303	0.057
120	0.211	0.052	0.401	0.068	0.298	0.057	0.336	0.064
ICS	4.12	0.99	6.26	1.52	5.19	1.25	5.59	1.34
MTCS	2.55	0.61	4.56	1.10	4.37	1.05	4.74	1.14

Table 4. Present experimental DCS, ICS and MTCS for excitation of the $C^1\Sigma^+$ state in units of 10^{-18} cm^2/sr and cm^2.

θ (°)	E_0 (eV)							
	12.5 eV	Error	15 eV	Error	17.5 eV	Error	20 eV	Error
10			1.49	0.51	1.24	0.31	1.70	0.396
15	0.490	0.162	1.11	0.21	0.749	0.171	1.386	0.249
20	0.353	0.084	0.68	0.13	0.486	0.088	0.962	0.173
25	0.234	0.045	0.451	0.086	0.377	0.068	0.589	0.106
30	0.167	0.032	0.320	0.061	0.323	0.058	0.488	0.088
40	0.167	0.032	0.217	0.041	0.371	0.067	0.349	0.063
50	0.095	0.018	0.191	0.036	0.367	0.066	0.544	0.098
60	0.077	0.015	0.184	0.035	0.342	0.062	0.409	0.074
70	0.090	0.017	0.152	0.029	0.310	0.056	0.294	0.053
80	0.088	0.017	0.145	0.028	0.252	0.045	0.210	0.038
90	0.052	0.010	0.155	0.029	0.239	0.043	0.212	0.038
100	0.048	0.009	0.131	0.025	0.188	0.034	0.325	0.059
110	0.048	0.009	0.122	0.023	0.195	0.035	0.353	0.064
120	0.068	0.013	0.098	0.019	0.151	0.027	0.273	0.049
ICS	1.24	0.34	2.46	0.61	3.46	0.76	4.75	1.15
MTCS	0.870	0.235	1.77	0.48	2.76	0.74	4.08	1.10

has proved to be useful for the present study which involves excitation to higher lying Rydberg states. Below, we discuss the scattering model used in the UKRMol calculation that employs a compact basis set including high angular momentum polarisation functions and two different models for the UKRMol+ calculation that employ a diffuse basis set.

3.1. UKRmol model

This model, which uses the large cc-pV6Z basis set but without augmentation of diffuse functions, was originally developed to study Feshbach resonances of CO molecule at its equilibrium bond distance of $R = 2.1323a_0$ (Dora and Tennyson 2019) and recently this has been extended to calculate the potential energy curves of several resonant states of CO^- anion (Dora and Tennyson 2020). This basis set was adequate to describe the valence as well as low lying Rydberg states of the target molecule, see table 1, and gave excellent results for resonance parameters as a function of bond distance, calculated in the R range from 1.7 a_0 to 2.38 a_0 (Dora and Tennyson 2020). However, for higher lying Rydberg states (in particular the $j^3\Sigma^+$ and $C^1\Sigma^+$ states) the calculated vertical excitation energies are too high (by 2.95 eV and 3.53 eV, respectively) in comparison to the experimental (adiabatic) values.

Here we briefly present the scattering model used in this calculation; details about this can be found in the above mentioned papers. The scattering wave function was represented

Table 5. Present experimental DCS, ICS and MTCS for excitation of the $E^1\Pi$ state in units of 10^{-18} cm^2/sr and cm^2.

θ (°)	E_0 (eV)							
	12.5 eV	Error	15 eV	Error	17.5 eV	Error	20 eV	Error
10			1.84	0.35	0.963	0.173	1.23	0.222
15	1.05	0.21	1.06	0.20	0.695	0.125	0.934	0.168
20	0.675	0.135	0.760	0.144	0.606	0.109	0.867	0.156
25	0.488	0.098	0.609	0.116	0.488	0.088	0.818	0.147
30	0.345	0.069	0.399	0.076	0.352	0.063	0.535	0.096
40	0.252	0.050	0.286	0.054	0.393	0.071	0.423	0.076
50	0.187	0.037	0.209	0.040	0.409	0.074	0.367	0.066
60	0.119	0.024	0.197	0.038	0.356	0.064	0.234	0.042
70	0.059	0.012	0.156	0.030	0.263	0.047	0.221	0.040
80	0.034	0.007	0.175	0.033	0.233	0.042	0.201	0.036
90	0.026	0.005	0.131	0.025	0.231	0.041	0.255	0.046
100	0.035	0.007	0.112	0.021	0.248	0.045	0.223	0.040
110	0.042	0.008	0.125	0.024	0.248	0.045	0.181	0.033
120	0.065	0.013	0.188	0.036	0.225	0.031	0.257	0.046
ICS	1.81	0.43	3.11	0.73	3.76	0.83	3.89	0.91
MTCS	1.07	0.26	2.57	0.60	3.21	0.71	3.27	0.77

Table 6. Present experimental DCS, ICS and MTCS for excitation of the $j^3\Sigma^+$ state in units of 10^{-18} cm^2/sr and cm^2.

θ (°)	E_0 (eV)							
	12.5 eV	Error	15 eV	Error	17.5 eV	Error	20 eV	Error
10			0.459	0.087	0.168	0.030	0.129	0.023
15	0.201	0.040	0.250	0.047	0.141	0.025	0.108	0.019
20	0.106	0.021	0.185	0.035	0.101	0.018	0.085	0.015
25	0.043	0.009	0.145	0.028	0.068	0.012	0.066	0.012
30	0.041	0.008	0.090	0.017	0.063	0.011	0.050	0.009
40	0.031	0.006	0.076	0.014	0.058	0.010	0.058	0.010
50	0.016	0.003	0.039	0.007	0.053	0.009	0.045	0.008
60	0.018	0.004	0.039	0.007	0.039	0.007	0.046	0.008
70	0.023	0.005	0.030	0.006	0.037	0.007	0.037	0.007
80	0.018	0.004	0.020	0.004	0.027	0.005	0.036	0.006
90	0.012	0.002	0.015	0.003	0.022	0.004	0.035	0.006
100	0.008	0.002	0.013	0.003	0.018	0.003	0.039	0.007
110	0.011	0.002	0.013	0.003	0.019	0.003	0.036	0.006
120	0.014	0.003	0.015	0.003	0.016	0.003	0.032	0.006
ICS	0.447	0.107	0.512	0.120	0.549	0.121	0.519	0.122
MTCS	0.249	0.060	0.275	0.065	0.346	0.076	0.444	0.104

by close-coupling expansion using 27 low-lying states of CO molecule. These states, in $C_{\infty v}$ symmetry, are the lowest 4 states of $^1\Sigma^+$, 2 of $^1\Sigma^-$, 4 of $^3\Sigma^+$, 3 of $^3\Sigma^-$, 5 of $^1\Pi$, 5 of $^3\Pi$, 2 of $^1\Delta$ and 2 of $^3\Delta$. The target molecular orbitals (MOs) needed for this calculation were obtained from MOLPRO package (Werner *et al* 2012) using the complete active space self-consistent-field (CASSCF) method using the cc-pV6Z Gaussian basis set. The active space corresponds to configurations generated by distributing 10 valence electrons in 10 valence MOs keeping the core electrons closed—in C_{2v} symmetry this is defined as: $(1a_1–2a_1)^4\,(3a_1–6a_1, 1b_1–3b_1, 1b_2–3b_2)^{10}$. An R-matrix sphere of radius $12a_0$ and continuum orbitals (represented using Gaussian type functions (Faure *et al* 2002)) with partial waves up to $\ell = 4$, have been used in the scattering calculation.

3.2. *UKRmol+ model*

The target models used in this work were constructed as an extension of the CASSCF model used in our previous work (Zawadzki *et al* 2020) which used the full valence active space $(1a_1–2a_1)^4\,(3a_1–6a_1, 1b_1–2b_1, 1b_2–2b_2)^{10}$ or (6, 2, 2, 0) and cc-pVQZ atomic basis.

In this work we performed calculations with two different models. An accurate description of Rydberg excited states requires inclusion of diffuse atomic basis functions and the corresponding Rydberg-like MOs in the active space. In this

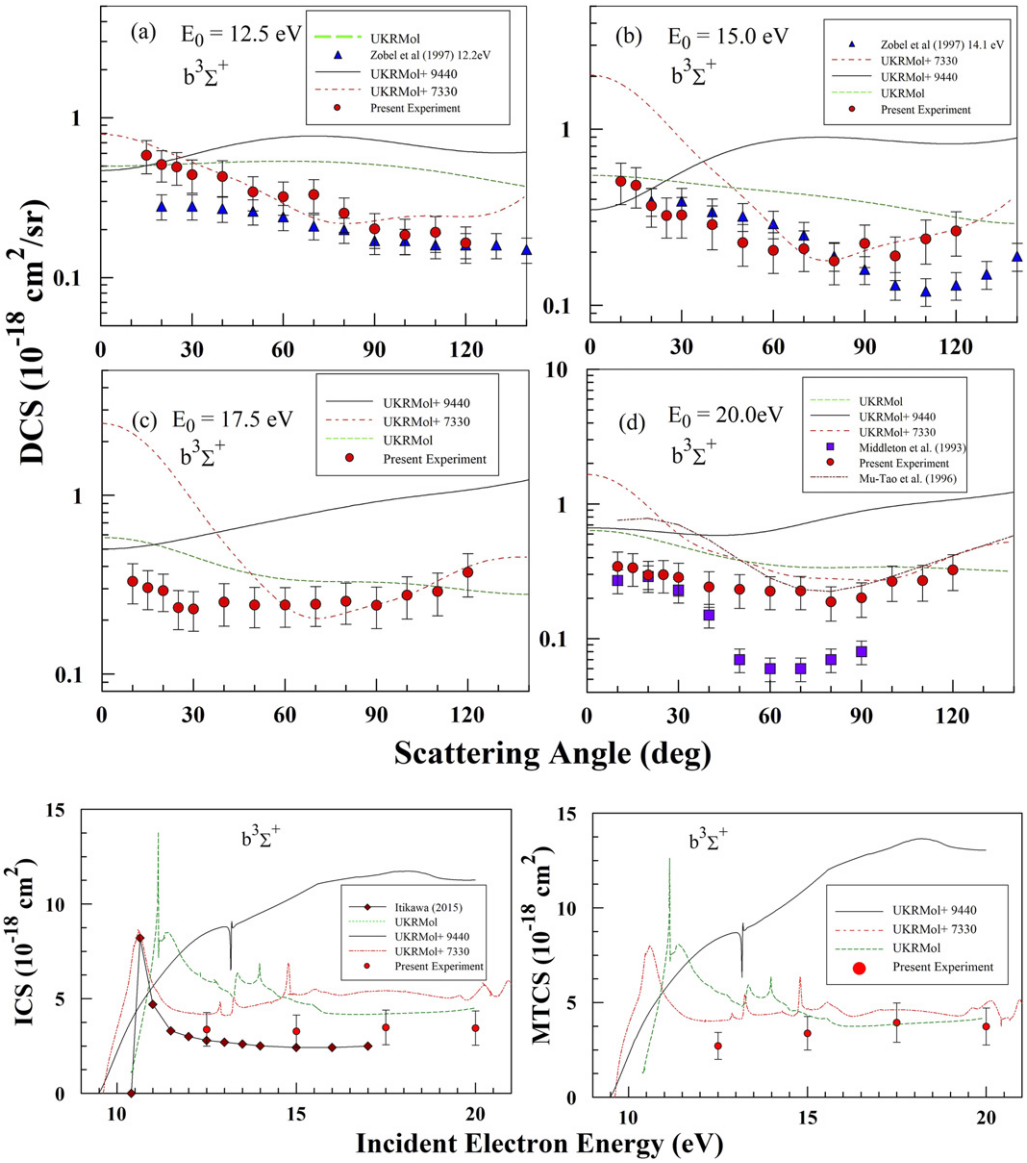

Figure 1. DCS and ICS, MTCS for electron impact excitation of the $b^3\Sigma^+$ state. Legend: solid red circles, present experiment; solid blue triangles, (Zobel *et al* 1995); solid purple squares, (Middleton *et al* 1993); solid black line, UKRMol+ 9440 model; staggered dashed red line, UKRMol+ 7330 model; small dashed line, UKRModel; brown line-connected diamonds, recommended ICSs of Itikawa (2015).

work we have used the aug-cc-pVQZ GTO basis and constructed two different target models.

In both cases the CASSCF target orbitals were obtained from MOLPRO (Werner *et al* 2012) using the above described GTO basis, the corresponding active spaces and state averaging procedure with equal weights. The averaging included a total of 10 C_{2v} states: 1–3 $^1A_1$, 1–2 $^1B_1$, 1–2 $^1B_2$, 1–3 $^3A_1$ which correspond to several low lying valence states and the five $C_{\infty v}$ Rydberg states investigated here. The averaging included both degenerate components of the Π states.

3.2.1. Model 7330. The first model, called 'UKRmol+ 7330', includes in the active space the additional orbitals $7a_1$ ($3s\sigma$), $3b_1$ ($3p\pi$) and $3b_2$ ($3p\sigma$) which are essential for description of the basic configurations of the Rydberg states of interest (Zawadzki *et al* 2020). Concretely the active space has the form $(1a_1–2a_1)^4$ $(3a_1–7a_1, 1b_1–3b_1, 1b_2–3b_2)^{10}$.

The scattering calculations based on this model employed a mixed B-spline (BTO) and GTO description of the continuum (Mašín *et al* 2020). The GTO part of the continuum basis used exponents optimized for radius of 10 Bohr. The B-spline basis comprised of 12 functions covering the radial range from 9 Bohr up to the R-matrix radius of 20 Bohr. Angular momenta up to $l = 5$ were included in both parts of the continuum basis. The deletion thresholds for orthogonalization of the continuum were set to 10^{-5}.

3.2.2. Model 9440. The second model, called 'UKRmol+ 9440', included additional 4 orbitals in the active space but keeps the first 4 orbitals of a_1 symmetry doubly occupied and has the form $(1a_1–4a_1)^8$ $(5a_1–9a_1, 1b_1–4b_1, 1b_2–4b_2)^6$.

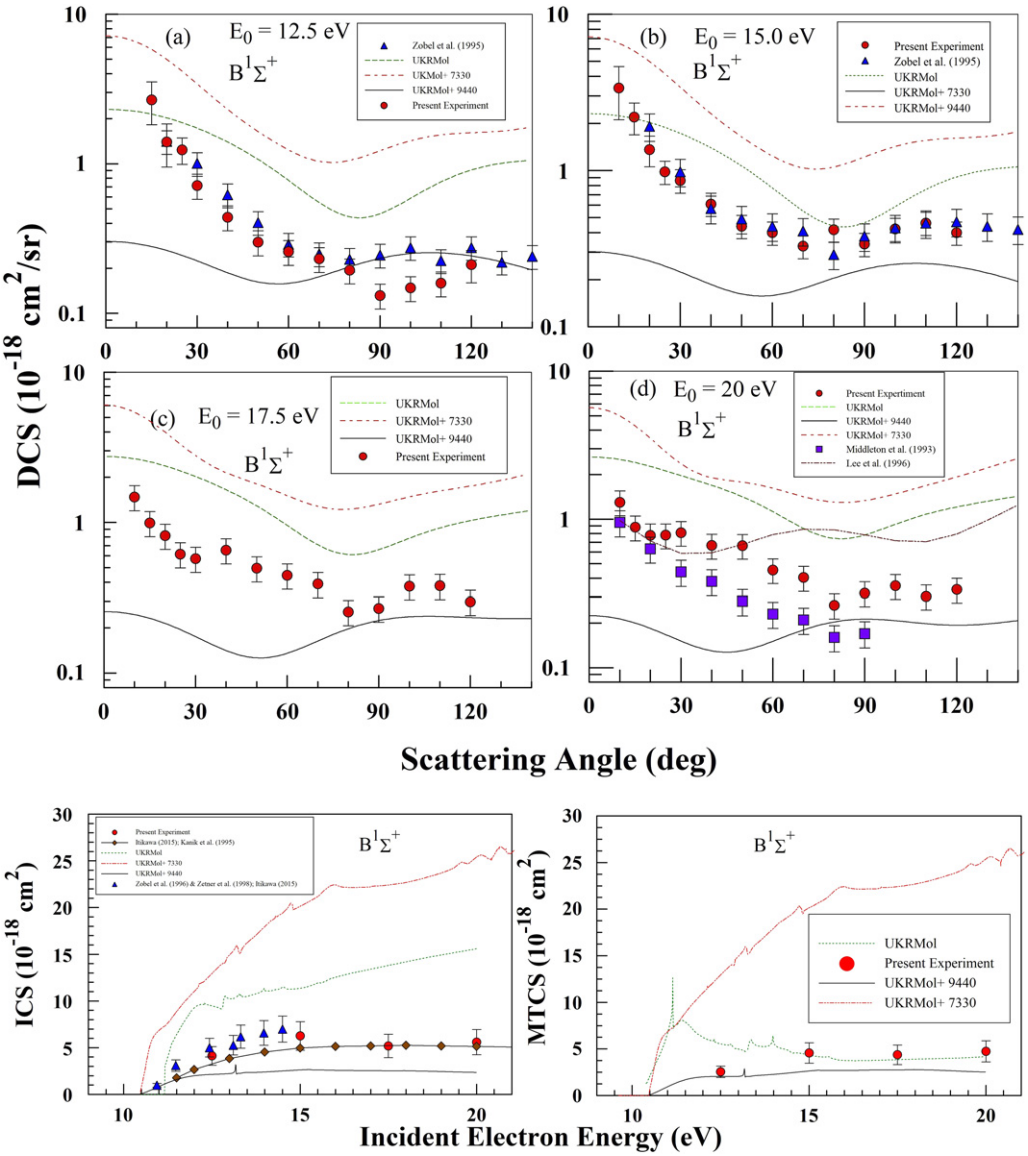

Figure 2. DCS and ICS, MTCS for electron impact excitation of the $B^1\Sigma^+$. Legend same as figure 1 except brown line-connected diamonds, Itikawa (2015) compilation of the emission measurements of Kanik *et al* (1995) and brown dot-dashed line distorted-wave approximation of Lee *et al* (1996) and the ICS solid blue triangles of the compilation by Zobel *et al* (1995) from Zobel *et al* (1995) and Zetner *et al* (1998).

In this model the continuum basis employed only GTOs. Their exponents were optimized for radius of 18 Bohr and angular momenta up to $l = 4$. R-matrix radius of 20 Bohr was used for the scattering calculation. We used quad precision to compute all molecular integrals (Mašín *et al* 2020) which allowed us to retain the whole continuum basis and thus ensure accurate description of the continuum up to the R-matrix boundary.

3.3. Comparison of target models

A comparison of the experimental and our calculated vertical excitation energies from the different target models is shown in table 1. In general the calculated results differ significantly with respect to each other with the smallest differences observed between models 7330 and 9440.

It is seen by comparing the UKRmol+ and model 7330 results that the vertical energies for the states $b^3\Sigma^+$ and $B^1\Sigma^+$, corresponding to occupation of the $3s\sigma$ orbital, are not significantly affected by the extension of the active space and inclusion of the diffuse functions in the atomic basis. Therefore those states probably have a dominant valence character. For all the other states the extension of the UKRmol+ models to models 7330 or 9440, which are more appropriate for description of Rydberg states, dramatically improves the vertical excitation energies and brings them down by several eV, in case of the j-state even by more than 10 eV, closer to agreement with experiment.

The C-state and j-state energies in both compact models UKRmol and UKRmol+ are in the worst disagreement with the experimental data, and are most improved in model 7330, suggesting that these two states have the strongest Rydberg character from the states studied here.

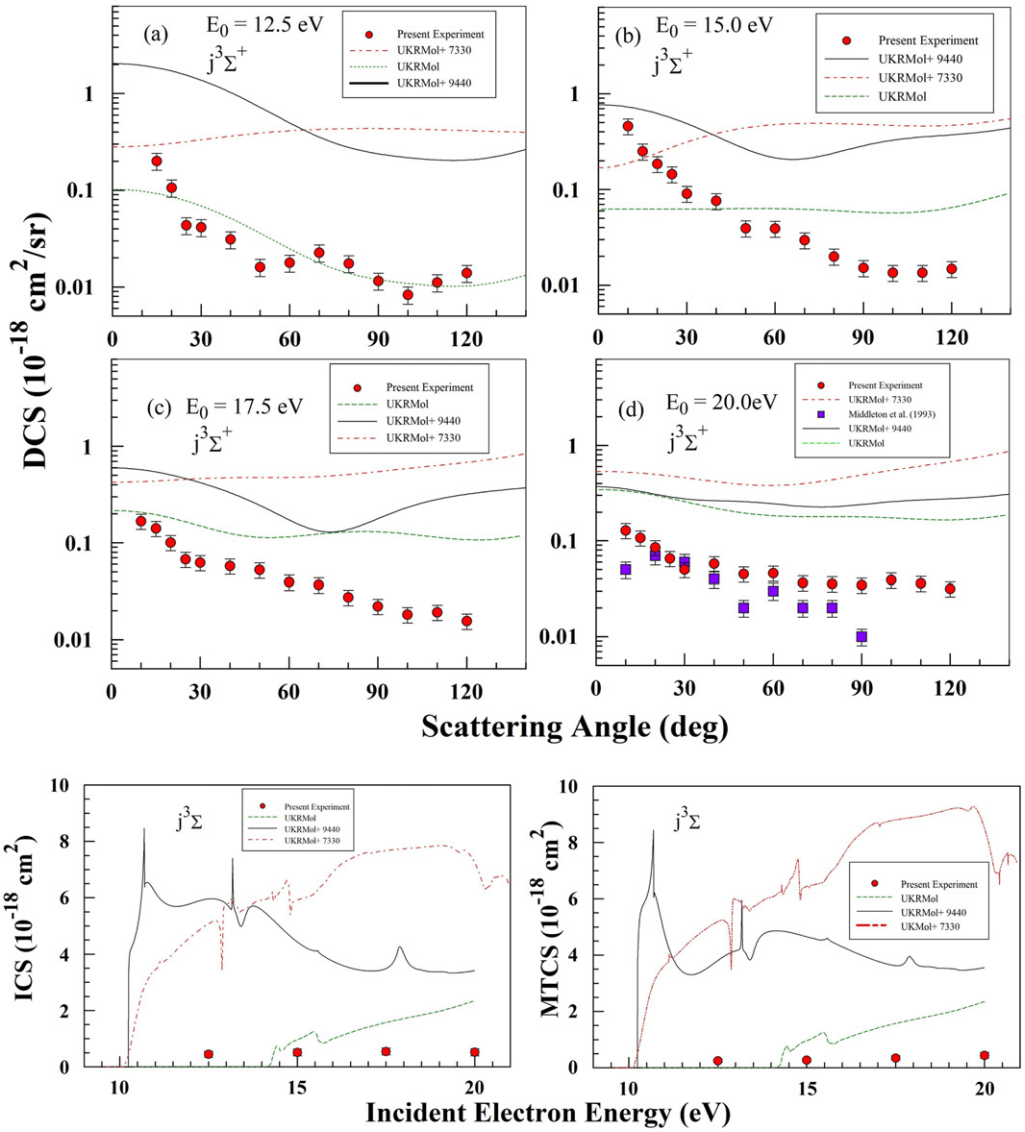

Figure 3. DCS and ICS, MTCS for electron impact excitation of the $j^3\Sigma^+$ state. Legend same as figure 1.

The vertical energies for model 7330 are less than 1 eV away from the experimental ones with exception of the j-state energy which is about 1.15 eV smaller than the experimental reference. Model 9440 is not in a better agreement with the experiment than model 7330. However, the choice of the active space affects the scattering calculations too and will be investigated below. Given the limitations of our approach to modelling electronic structure we consider models 7330 and UKRmol to be in a good agreement with experiment.

Description of the Rydberg states by the compact valence UKRmol+ model is clearly inadequate and therefore this model needs to be reconsidered in the future as a viable method to use for modelling impact excitation of CO Rydberg states.

4. Results and discussion

Our experimental results are summarised in the tables 2–6. They are compared with our present R-matrix calculations and the results of other available experiments and theoretical models. Figure 1 shows the DCS, ICS and MTCS for the electron impact excitation of $b^3\Sigma^+$ ($2\,^3\Sigma^+$) state of CO. Figure 2 shows the DCS, ICS and MTCS for the $B^1\Sigma^+$ ($2\,^1\Sigma^+$) state. Figure 3 shows the DCS, ICS and MTCS for the $j^3\Sigma^+$ ($3\,^3\Sigma^+$) state. Figure 4 shows the DCS, ICS and MTCS for the $C^1\Sigma^+$ ($3\,^1\Sigma^+$) state. Figure 5 shows the DCS, ICS and MTCS for the excitation of the $E^1\Pi$ ($2\,^1\Pi$) state. Tables 2–6 display the experimental DCS, ICS and MTCS for the excitation of $b^3\Sigma^+$ ($2\,^3\Sigma^+$), $B^1\Sigma^+$ ($2\,^1\Sigma^+$), $C^1\Sigma^+$ ($3\,^1\Sigma^+$), $E^1\Pi$ ($2\,^1\Pi$) and $j^3\Sigma^+$ ($3\,^3\Sigma^+$) states, respectively.

In figure 1, for the excitation of the $b^3\Sigma^+$ state we see good agreement at E_0 of 12.5 eV between the present experimental results and those of Zobel *et al* (1995) as well as with the UKRMol+ 7330 model. This good agreement is similarly observed at E_0 of 15 eV, although the UKRMol+ 7330 theory does not show good agreement towards small θ at this E_0 and higher ones. For the ICS agreement with the recommended ICSs of Itikawa is good, whereas the

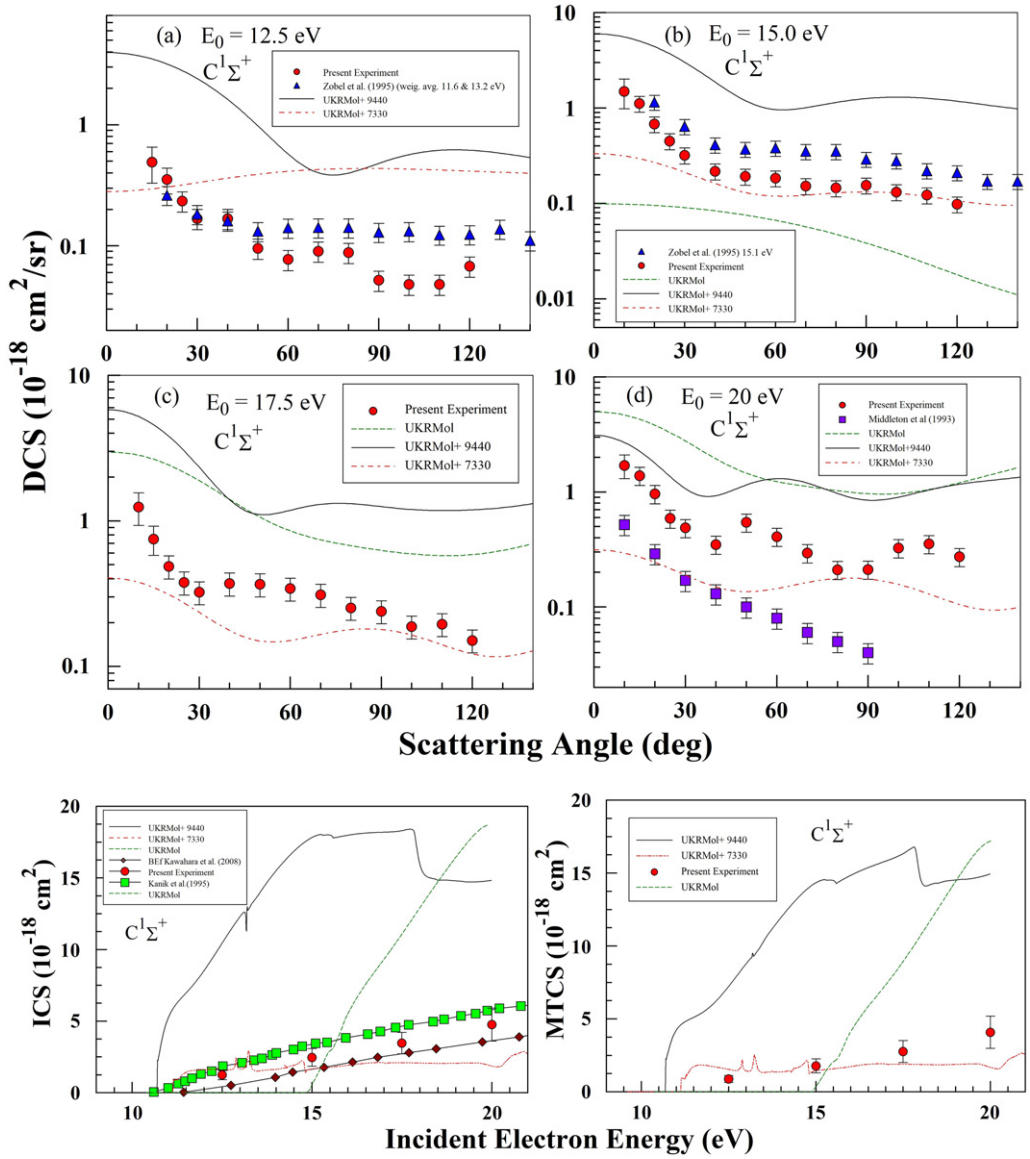

Figure 4. DCS and ICS, MTCS for excitation of the $C^1\Sigma$ state. Legend same as figure 1 except brown line-connected diamonds (Itikawa 2015) of the compilation of (Itikawa 2015) of the BEf scaling results of the CO emission measurements of Kawahara *et al* (2008). The green line-connected squares are the compilation of Itikawa (2015) of the CO emission measurements of Kanik *et al* (1995).

UKRMol and UKRMol+ ICSs are higher especially the UKRMol+ 9440 ICS values. For MTCS the present experimental results are in satisfactory agreement at all E_0 with UKRMol+ 7330 and UKRMol; the UKRMol+ 9440 is however both in qualitative and quantitative disagreement with experiment. At $E_0 = 20$ eV we obtain a satisfactory agreement with the Distorted-Wave DCSs calculations of Lee *et al* (1996) at large θ, but not at the smaller θ. Both the UKRMol+ 7330 and UKRMol show steep rises of the ICS and consequently MTCS at a nominal threshold of $E_0 \approx 10$ eV, but notably not the UKRMol+ 9440 model which shows a gradual rise of the ICS/MTCS near threshold.

Figure 2, for the $B^1\Sigma^+$ results, we find very good agreement between the present experiment and the DCSs of Zobel *et al* (1995) except that our DCSs are notably lower at around $\theta \approx 90°$. At $E_0 = 20$ eV, the DCSs of Middleton *et al* (1993) are qualitatively in good agreement with the present experiment, but significantly lower. Best quantitative agreement for the $B^1\Sigma^+$ DCSs is obtained with the UKMol model although none of the models provide a good agreement. For the ICSs of the $B^1\Sigma^+$ very good agreement is found between the present experimental results and those of Zobel *et al* (1995) compiled by Itikawa (2015) and of the electron impact emission results of Kanik *et al* (1995) also compiled in Itikawa (2015). Better quantitative agreement is found with the present experimental MTCSs and those of the UKRMol+ 9440 and the UKRMol models.

For the $j^3\Sigma^+$ results in figure 3, we find a good agreement with DCS from the UKRMol model at $E_0 = 12.5$ eV, but the UKRMol+ models give too high DCSs. For the other E_0 values disagreement is large between the experiment and

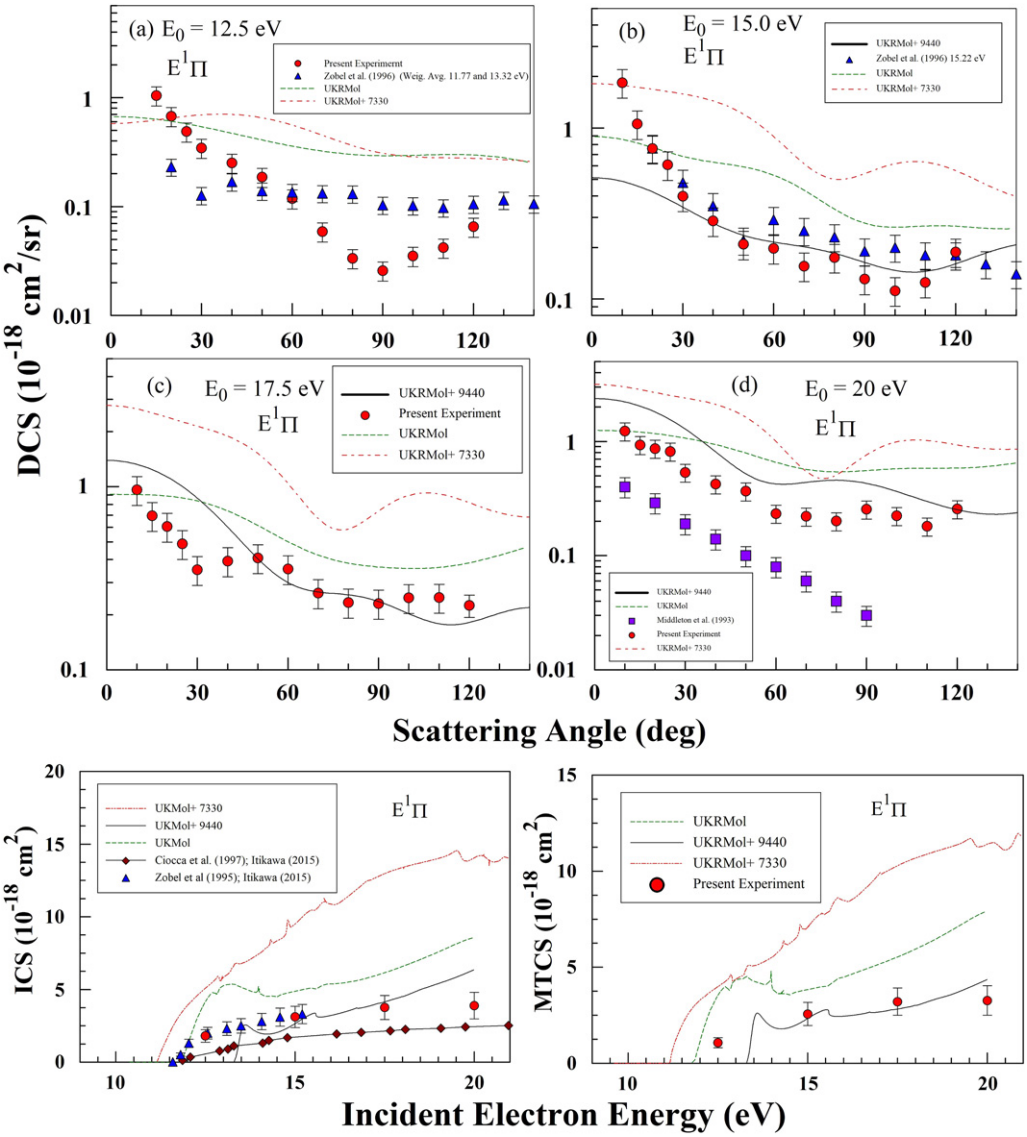

Figure 5. DCS and ICS, MTCS for excitation of the $E^1\Pi$ state. Legend same as figure 1 except solid blue triangles (Itikawa 2015) compilation of Zobel *et al* (1995), brown line-connected diamonds, (Itikawa 2015) compilation of the CO emission measurements of Ciocca *et al* (1996).

the UKRMol+ and UKRMol models. This also goes with the experimental ICSs and MTCSs which are markedly lower than theory.

Similar disagreements are to be seen in figure 4 for the DCS for $C^1\Sigma^+$ state with best agreement between UKRmol+ 7330 theory and the present experiment at E_0 of 15.0 eV, 17.5 eV and 20 eV. The present experimental results and those of Zobel *et al* (1995) and Middleton *et al* (1993) show good qualitative agreement with each other, but significant differences between them exist, especially with Middleton *et al* (1993). For the ICSs the present results are in-between the values of Kawahara *et al* (2008) and Kanik *et al* (1995) both compiled by Itikawa (2015).

For excitation of the $E\ ^1\Pi$ state DCSs in figure 5 we find disagreement between the present experiment and Zobel *et al* (1995) at $E_0 = 12.5$ eV, but this could be understood from the fact that their data had to be averaged between E_0 of 13.3 eV and 11.7 eV. Nevertheless at the E_0 of 15 eV agreement between the two experimental DCSs is very good and the agreement with the UKRMol+ 9440 model is also very good at non-forward angles and $E_0 > 12.5$ eV. At $E_0 = 20$ eV we find disagreement between the present experimental DCSs and those of Middleton *et al* (1993) which are significantly lower in magnitude than theoretical models. The ICSs of the present experiment and those of Zobel *et al* (1995) are in very good agreement but are higher than the emission measurements of Ciocca *et al* (1996), both experiments complied by Itikawa (2015). Agreement of the present experimental ICSs and MTCSs with the UKRMol+ 9440 model is very good except that the calculated threshold is too high at $E_0 = 13.31$ eV compared to the experimental threshold of $\approx$11.6 eV.

Overall agreement of DCSs between experiments is good for scattering energies (E_0) of 12.0 eV and 15.0 eV, but unsatisfactory at 20 eV. The experimental ICSs and MTCSs are

found to be in reasonable agreement with other experimental ICSs and MTCSs, although at variance by ≈25%–30%. Agreement with theoretical models is occasionally good, but mostly unsatisfactory, and also is reflected in the variance between the theoretical models themselves. Clearly, much needs to be improved as far as the modeling aspects are concerned, but some improvement in experimental DCSs is required although this is limited to the fact that the energy loss features of CO heavily overlap for the triplet states. However the energy loss features are more open for the singlets, and thus the experimental DCSs should be better for the $B^1\Sigma^+$, $C^1\Sigma^+$ and $E^1\Pi$ states.

5. Conclusions

Despite the occasionally excellent agreement between the experimental and our calculated target vertical excitation energies, the theoretical scattering DCS results are mostly inaccurate when compared against the present experiment. Therefore reproducing the vertical excitation energy in the calculation is most likely not the critical parameter when it comes to description of excitation of Rydberg states by electron impact and the role of other properties of the Rydberg states needs to be investigated in the future.

Accurate modelling of electronic structure of Rydberg states of CO can be achieved using the R-matrix approach by modelling the system as comprising of a CO^+ core and one electron coupled to it while making use of the division of space to describe the long-range (Rydberg) part of the wave function using the one-electron R-matrix outer region (Chakrabarti and Tennyson 2006). However, a simultaneous modelling of the Rydberg states using the aforementioned technique and inclusion of one additional (scattering) electron would be computationally equivalent to description of interaction of two electrons in the continuum coupled to a multi-electron core; this is not possible in the current implementation of the R-matrix method.

One could argue that inclusion of the diffuse atomic functions and Rydberg orbitals, impossible in the older (UKRmol version) of the R-matrix code, would lead to an improvement of the scattering results but that is not the case either. This opens the possibility that nuclear motion and vibronic coupling is involved and its role should be investigated in the future too. Except for rather simple systems (Meltzer *et al* 2020) and despite the recent significant progress in the extension of capabilities of the R-matrix codes (Mašín *et al* 2020), electron molecule collisions involving electronic excitation to Rydberg states remain challenging.

Acknowledgments

MZ acknowledges the Fulbright Program for a senior fellowship to conduct this work at California State University Fullerton. MAK and MZ acknowledge support from National Science Foundation research Grants: NSF-RUI AMO 1606905 and 1911702. ZM acknowledges support of the Czech Science Foundation (Project GA CR Junior No. 20-15548Y) and support of the PRIMUS Project 20/SCI/003 of the Charles University. This work was supported by the Ministry of Education, Youth and Sports of the Czech Republic through the e-INFRA CZ (ID: 90140). JT thanks the UK EPSRC for funding under the UK-AMOR Project, Grant EP/R029342/1 and AD acknowledges SERB, Govt. of India Grant Number EMR/2017/003179.

Data availability statement

All data that support the findings of this study are included within the article (and any supplementary files).

ORCID iDs

Mateusz Zawadzki https://orcid.org/0000-0003-3912-2876
Murtadha A Khakoo https://orcid.org/0000-0002-8628-7131
Zdeněk Mašín https://orcid.org/0000-0001-9382-4655
Amar Dora https://orcid.org/0000-0002-8167-882X
Russ Laher https://orcid.org/0000-0003-2451-5482
Jonathan Tennyson https://orcid.org/0000-0002-4994-5238

References

Allan M 1989 *J. Electron Spectrosc. Relat. Phenom.* **48** 219–351
Brunger M J and Buckman S J 2002 *Phys. Rep.* **357** 215–458
Campbell L, Allan M and Brunger M J 2011 *J. Geophys. Res.: Space Phys.* **116** A9
Carr J M *et al* 2012 *Eur. Phys. J.* D **66** 58
Cartwright D C, Chutjian A, Trajmar S and Williams W 1977 *Phys. Rev.* A **16** 1013–40
Chakrabarti K and Tennyson J 2006 *J. Phys. B: At. Mol. Opt. Phys.* **39** 1485–97
Ciocca M, Kanik I and Ajello J M 1996 *Phys. Rev.* A **55** 3547–56
Dora A and Tennyson J 2019 *Quantum Collisions and Confinement of Atomic and Molecular Species, and Photons* ed P C Deshmukh, E Krishnakumar, S Fritzsche, M Krishnamurthy and S Majumder vol 230 (Berlin: Springer) pp 48–59
Dora A and Tennyson J 2020 *J. Phys. B: At. Mol. Opt. Phys.* **53** 195202
Faure A, Gorfinkiel J D, Morgan L A and Tennyson J 2002 *Comput. Phys. Commun.* **144** 224–41
Ghenai C 2010 *Adv. Mech. Eng.* **2** 342357
Gibson J C, Morgan L A, Gulley R J, Brunger M J, Bundschu C T and Buckman S J 1996 *J. Phys. B: At. Mol. Opt. Phys.* **29** 3197–214
Huber K P and Herzberg G 1950 *Molecular Spectra and Molecular Structure: Spectra of Diatomic Molecules* (Princeton, NJ: Van Nostrand-Reinhold)
Huber K P and Herzberg G 1979 *Constants of Diatomic Molecules* (Princeton, NJ: Van Nostrand-Reinhold)
Hughes M, James K E, Childers J G and Khakoo M A 2003 *Meas. Sci. Technol.* **14** 841–5
Itikawa Y 2015 *J. Phys. Chem. Ref. Data* **44** 013105
Kaltschmitt T and Deutschmann O 2012 *Adv. Chem. Eng.* **41** 1–64
Kanik I, James G K and Ajello J M 1995 *Phys. Rev.* A **51** 2067–74
Kawahara H, Kato H, Hoshino M, Tanaka H and Brunger M J 2008 *Phys. Rev.* A **77** 012713
Khakoo M A, Beckmann C E, Trajmar S and Csanak G 1994 *J. Phys. B: At. Mol. Opt. Phys.* **27** 3159–74

Lee M-T, Machado A M, Fujimoto M M, Machado L E and Brescansin L M 1996 *J. Phys. B: At. Mol. Opt. Phys.* **29** 4285–301
Mašín Z, Benda J, Gorfinkiel J D, Harvey A G and Tennyson J 2020 *Comput. Phys. Commun.* **249** 107092
Mazeau J, Schermann C and Joyez G 1975 *J. Electron Spectrosc. Relat. Phenom.* **7** 269–79
Meltzer T, Tennyson J, Mašín Z, Zammit M C, Scarlett L H, Fursa D V and Bray I 2020 *J. Phys. B: At. Mol. Opt. Phys* **53** 145204
Middleton A G, Brunger M J and Teubner P J O 1993 *J. Phys. B: At. Mol. Opt. Phys.* **26** 1743–59
Nakano K, Kodama S, Permana Y and Nozaki K 2009 *Chem. Commun.* **45** 6970–2
Press W H, Vetterling S A T W V and Flannery B P 1988 *Numerical Recipes in C++. The Art of Scientific Computing* 2nd edn (Cambridge: Cambridge University Press)
Ralphs K, Serna G, Hargreaves L R, Khakoo M A, Winstead C and McKoy V 2013 *J. Phys. B: At. Mol. Opt. Phys.* **46** 125201
Sakurai T and Yokoyama A 2000 *J. Nucl. Sci. Technol.* **37** 814–20
Swanson N, Celotta R J, Kuyatt C E and Cooper J W 1975 *J. Chem. Phys.* **62** 4880–8
Tanaka H, Srivastava S K and Chutjian A 1978 *J. Chem. Phys.* **69** 5329–33
Trajmar S, Register D F and Chutjian A 1983 *Phys. Rep.* **97** 221–356
Varela K, Hargreaves L R, Ralphs K, Khakoo M A, Winstead C, Mckoy V, Rescigno T N and Orel A E 2015 *J. Phys. B: At. Mol. Opt. Phys.* **48** 115208
Werner H-J, Knowles P J, Knizia G, Manby F R and Schütz M 2012 *Wiley Interdiscip. Rev.-Comput. Mol. Sci.* **2** 242–53
Zawadzki M, Khakoo M A, Voorneman L, Ratkovic L, Mašín Z, Houfek K, Dora A, Russ L and Tennyson J 2020 *J. Phys. B: At. Mol. Opt. Phys.* **53** 165201
Zetner P W, Kanik I and Trajmar S 1998 *J. Phys. B: At. Mol. Opt. Phys.* **31** 2395–413
Zobel J, Mayer U, Jung K, Ehrhardt H, Pritchard H, Winstead C and Mckoy V 1995 *J. Phys. B: At. Mol. Opt. Phys.* **28** 839–56
Zobel J, Mayer U, Jung K and Ehrhardt H 1996 *J. Phys. B: At. Mol. Opt. Phys.* **29** 813–38